Wet-Chemical Route for the Preparation of Lead Zirconate: An Amorphous Carbon- and Halide-Free Precursor Synthesized by the Hydrogen Peroxide Based Route

Emerson R. Camargo, Monica Popa, Johannes Frantti, and Masato Kakihana*

Materials and Structures Laboratory, Tokyo Institute of Technology, Nagatsuta 4259, Midori-ku, Yokohama 226-8503, Japan

Received April 12, 2001. Revised Manuscript Received July 9, 2001

$PbZrO_3$ (PZ) nanoparticles were synthesized through a halide- and organic-free hydrogen peroxide method at 700 °C for 2 h. Stoichiometric amounts of zirconyl nitrate and lead nitrate were dissolved in a diluted H_2O_2 (aqueous) solution, which was slowly dropped into a solution of H_2O_2 and NH_3 (pH = 11). The precipitate of Pb−Zr, obtained from an exothermic oxy-reduction reaction, was filtered and washed to eliminate all nitrate ions. The precipitate was dried, ground, and calcined between 300 and 1000 °C, for 5 min to 8 h. Tetragonal, lead-rich zirconia solid solution (t-Z) was identified by thermogravimetry−differential thermal analysis, X-ray diffraction, and Raman spectroscopy as an intermediate phase during the calcination process, followed by the crystallization of the orthorhombic PZ phase. The average particle size was estimated to be 50 nm from scanning electron microscopy pictures. The change in the amount of residual t-Z phase in PZ powders was estimated from the Raman spectra.

1. Introduction

Synthesis of lead-based oxides has been extensively studied because of the wide range of technological and industrial applications of these compounds. For instance, lead−zirconate−titanate (PZT) ceramics show unique microwave-dielectric,[1] pyroelectric, and piezoelectric properties.[2,3] Lead zirconate ($PbZrO_3$, PZ) has been reported as a potential material for energy storage.[4] The use of the conventional solid-state reaction technique for the preparation of PZ requires a high temperature, often resulting in powders with undesirable characteristics such as large particle size, broad distribution of the particle size, partially sintered agglomerates, and low chemical homogeneity due to the volatilization of lead. On the other hand, wet-chemical methods can be excellent techniques for the synthesis of pure and highly reactive multicomponent powders.[5−8]

Several wet-chemical methods have been reported for the synthesis of PZ, e.g., coprecipitation, hydrothermal synthesis, sol−gel synthesis, and microemulsion routes.[9−12] Another method, known as the "peroxide based route" (PBR), has been widely used in the synthesis of alkaline-earth-metal titanates and stannates, usually using chlorides as cation source.[13] Recently, Camargo and coworkers[14,15] developed a new PBR free from halides and organics for the synthesis of $PbTiO_3$, which can be called the "oxidant−peroxo method", based on the oxidation−reduction reaction between the Pb(II) ion and a water-soluble titanium−peroxide complex at high pH. The major advantages of this method over the previously reported PBR are (i) its simple experimental procedure that allows work under ambient atmosphere, (ii) the use of aqueous solvents and starting reagents that can be easily and safely handled, (iii) the total absence of organics and halides, and (iv) nongeneration of the toxic and corrosive HCl gas during the process. Here, we report the synthesis of orthorhombic PZ nanoparticles using the new oxidant−peroxo method approach of the PBR. Raman spectroscopy and X-ray diffraction (XRD) revealed an intermediate tetragonal lead-rich zirconia solid solution (t-Z) phase at low temperature. Raman peaks were used to estimate the change in the relative

* To whom correspondence should be addressed. Fax: +81 45 924 5309. E-mail: kakihana@rlem.titech.ac.jp.

(1) Lanagan, M. T.; Kim, J. H.; Jang, S.-J.; Newnham, R. E. *J. Am. Ceram. Soc.* **1988**, *77*, 311.
(2) Jaffe, B.; Cook, W. R.; Jaffe, H. *Piezoelectric ceramics*; Academic Press: London, 1971.
(3) Fujishita, H.; Shiozaki, Y.; Achiwa, N.; Sawaguchi, E. *J. Phys. Soc. Jpn.* **1982**, *51*, 3582.
(4) Singh, K. *Ferroelectrics* **1989**, *94*, 433.
(5) Camargo, E. R.; Kakihana, M.; Longo, E.; Leite, E. R *J. Alloys Compd.* **2001**, *314*, 140.
(6) Leite, E. R.; Paris, E. C.; Longo, E. *J. Am. Ceram. Soc.* **2000**, *83*, 1539.
(7) Kakihana, M. *J. Sol-Gel Sci. Technol.* **1996**, *6*, 5.
(8) Lakeman, C. D. E.; Payne, D. A. *Mater. Chem. Phys.* **1994**, *38*, 305.
(9) Okazaki, K.; Yoshioka, T.; Takahashi, K. *J. Ceram. Assoc. Jpn.* **1965**, *73*, 17.
(10) Kakegawa, K.; Mohri, J.; Shirasaki, S.; Takashi, K. *J. Am. Ceram. Soc.* **1984**, *67*, C-2.
(11) Ibrahim, D. M.; Hennicke, H. W. *Trans. J. Br. Ceram. Soc.* **1981**, *80*, 18.
(12) Ishida, K.; Hirota, K.; Yamaguchi, O.; Kume, H.; Inamura, S.; Miyamato, H. *J. Am. Ceram. Soc.* **1994**, *77*, 1391.
(13) Pfaff, G. *Mater. Lett.* **1995**, *24*, 393
(14) Camargo, E. R.; Kakihana, M. *Chem. Mater.* **2001**, *13*, 1181.
(15) Camargo, E. R.; Frantti, J.; Kakihana, M. *J. Mater. Chem.* **2001**, *11*, 1875.

10.1021/cm010326m CCC: $20.00
Published on Web 09/20/2001

Table 1. Reagents Used in the Synthesis of PZ Powders

material	purity (%)	composition	origin
zirconyl nitrate	97	$ZrO(NO_3)_2$	Wako Pure Chemicals, Japan
lead nitrate	99.9	$Pb(NO_3)_2$	Wako Pure Chemicals, Japan
hydrogen peroxide (solution)	>99.5	H_2O_2 (34%)	Tomiyama High Purity Chemicals, Japan
ammonia (solution)	>99.5	NH_3 (28%)	ELM, Japan

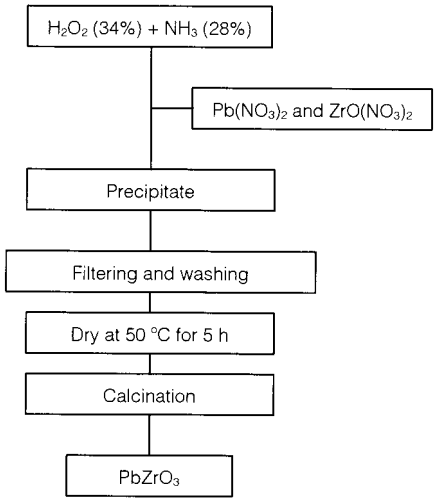

Figure 1. Flowchart for the preparation of $PbZrO_3$ through the peroxide based route.

amount of the t-Z phase in PZ powders as a function of the calcination temperature.

2. Experimental Section

2.1. Synthesis. Figure 1 shows the flowchart for the PZ synthesis, and the reagents are listed in Table 1. A stoichiometric aqueous solution of $Pb(NO_3)_2$ and $ZrO(NO_3)_2$ (100 mL) was prepared, with a total cation concentration of 0.6 mol L^{-1}, and molar ratio [Pb]:[Zr] = 1:1, followed by the addition of H_2O_2 (20 mL, 34%). A solution of H_2O_2 (80 mL, 34%) and NH_3 (20 mL, 28%) was prepared and stirred in an ice bath. When the Pb−Zr solution was slowly dropped into the H_2O_2–NH_3 solution, an exothermic reaction happened immediately with gas evolution and an orange precipitate was formed. After the addition of all Pb−Zr solution, the precipitate was filtered and washed with aqueous NH_3 (10%) to eliminate the nitrate ions. All lead and zirconium cations were precipitated, with a yield of approximately 100%. The washed precipitate was dried at 50 °C for 5 h and ground, and amounts of 0.50 g of the dry precipitate were calcined between 300 and 1000 °C for 5 min, 1 h, 2 h, and 8 h in a closed alumina boat, with a heating rate of 10 °C min^{-1}.

2.2. Characterization. A 6 mg sample of the dry precipitate was characterized by thermal analysis (TG−DTA 2000/Control model TAPS-1000, MAC-Science, Japan) in air between 30 and 800 °C, with a heating rate of 2 °C min^{-1}, using an Al_2O_3 crucible and α-Al_2O_3 as DTA reference. The powder morphology and the microstructure as well as the qualitative analysis of the samples were determined by scanning electron microscopy (SEM) (Hitachi S-4500 scanning microscope, Japan) equipped with an energy-dispersive X-ray spectrometer. XRD measurements were carried out using the MAC Science diffractometer (model MXP^{3VA}). A Cu Kα doublet (1.540562 and 1.544390 Å) was used for recording XRD patterns from the samples at room temperature. XRD intensities were recorded at 2θ angles between 5° and 95° with an angular velocity of 0.25 deg min^{-1}. The XRD pattern from the powder calcined at 900 °C for 2 h was collected with a step scan size of 0.02°, a step counting time of 10 s, and a 2θ range between 10° and 90°. Visible laser light (514.532 nm) was used for Raman measurements. The spectrometer used was the Jobin Yvon/Atago Bussan T64000 model with a liquid nitrogen cooled CCD detector. The resolution of the Raman spectrometer was about 1 cm^{-1}. The room-temperature spectra between 15 and 1000 cm^{-1} were measured using a triple monochromator with a grating of 1800 grooves mm^{-1}. All measurements were carried out under the microscope (laser spot diameter 1−2 μm) at a backscattering geometry. The power of the laser beam on the samples was adjusted to 10 mW, and the acquisition time was 10 s. The intensities of the Raman peaks (modeled with a Voigt function) were estimated using a commercial curve-fit program.[16]

3. Results and Discussion

3.1. Formation of the Pb−Zr Precipitate. Although several oxides have been prepared through the traditional PBR by the precipitation of alkaline-earth-metal salts of peroxo complexes,[13] the oxidation of lead in the presence of hydrogen peroxide at alkaline pH (see eq 1) is a serious obstacle to the preparation of lead based compounds via this technique, since it is impossible to obtain salts of peroxo complexes and Pb(II).

$$Pb(OH)_4^{2-} + H_2O_2 \rightarrow PbO_2 + 2H_2O + 2OH^- \quad (1)$$

Camargo and co-workers[14,15] developed a technique to prepare $PbTiO_3$ by applying eq 1 to obtain an amorphous and stoichiometric precipitate of lead and titanium from a water solution of the titanium−peroxo complex. A stable aqueous solution of zirconyl−peroxo complexes can also be synthesized by dissolving zirconyl ions in a diluted solution of H_2O_2 (eq 2).

$$ZrO^{2+} + H_2O_2 \rightarrow ZrO(O_2)H^+ + H^+ \quad (2)$$

When the pH is increased, the zirconyl−peroxo complex acts as an oxidizer, similarly to H_2O_2, raising the oxidation state of lead from Pb(II) to Pb(IV) (eq 3). As a result, a fine and highly reactive amorphous Pb−Zr precipitate is formed. This precipitate is free from undesirable halides and can be calcined at low temperature to obtain pure $PbZrO_3$.

$$ZrO(O_2)H^+ + Pb(OH)_4^{2-} \rightarrow PbO_2 + ZrO_2 + OH^- + 2H_2O \quad (3)$$

3.2. Thermogravimetry−Differential Thermal Analysis (TG−DTA) and Scanning Electron Microscopy−Energy-Dispersive X-ray Spectroscopy (SEM−EDS). Figure 2 shows TG and DTA curves of the dry precipitate. The TG curve revealed a continuous weight loss of 17.8%, over the range between 30 and 500 °C. Above 500 °C, there was no detectable mass change. In the DTA curve, a broad exothermic peak (1) was observed, starting at 218 °C and having maximum intensity at 365 °C. This peak was directly related to the continuous weight loss observed in the TG curve and

(16) PeakFit, version 4, Jandel Scientific Software, 1995.

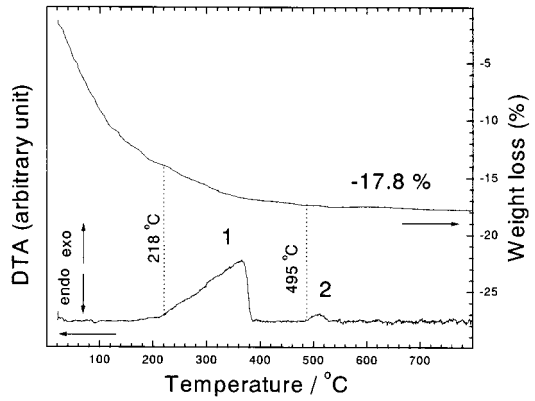

Figure 2. TG−DTA curves of the dry precipitate, between 30 and 800 °C, with a heating rate of 2 °C min^{-1}. The sample (mass 6 mg) was in an alumina crucible.

could be associated with the formation of the metastable zirconia phase. There was a second small and quite symmetric exothermic peak (2) between 495 and 530 °C. No significant weight loss was observed during this second event, which was associated with the PZ formation (see Figure 4). The results are in agreement with other reported data. Aoyama[17] found a metastable lead-rich zirconia solid solution during the synthesis of PZ using a coprecipitation method, characterized by an exothermic peak in the range between 450 and 510 °C, followed by a second exothermic peak at higher temperature.

The structural characterization was completed by microstructural studies using SEM and elemental analysis of the powders by using EDS. Figure 3 shows the sequence of the SEM images: (a) the dry amorphous precipitate, (b) the powder calcined at 500 °C for 2 h, and (c) the powder calcined at 700 °C for 2 h. All powders showed similar microstructures, good homogeneity, and a fine and uniform particle size. The results revealed an average grain size on the nanometric scale of about 50 nm. An interesting aspect to mention is that the samples maintained a spherical shape despite the increase in the calcination temperature. The ratio between lead and zirconium ions (Zr:Pb = 1.2 ± 0.1, in atomic percentage) was calculated from the EDS analysis for all powders. The EDS analysis for the PZ sample, as a result of the average of values taken from 10 distinct regions of the sample, showed that the particles consisted of the PZ phase. A small excess of zirconium due to the PbO_2 segregation was detected by EDS; however, the Zr:Pb ratio in different particles was nearly constant, which we believe is due to the uniform distribution of the cations.

3.3. X-ray Diffraction Characterization. Pure lead zirconate with an orthorhombic phase was obtained. Unit cell dimensions (a = 1.1784 nm, b = 0.8231 nm, and c = 0.5884 nm) were calculated from the XRD pattern of the powder calcined at 900 °C for 2 h. It is possible to observe from the XRD patterns of Figure 4 the amorphous nature of the dry precipitate, curve a, and the phase evolution when the precipitate was calcined for 2 h, curves b−f. Diffraction peaks indicated by solid squares in Figure 4 correspond to the PbO_2 phase, consistent with eq 3. The broad peaks, probably due to the small crystal size, in the XRD pattern of the powder calcined at 500 °C, Figure 4c, were assigned to the t-Z phase,[18,19] with characteristic peaks at 29°, 34°,

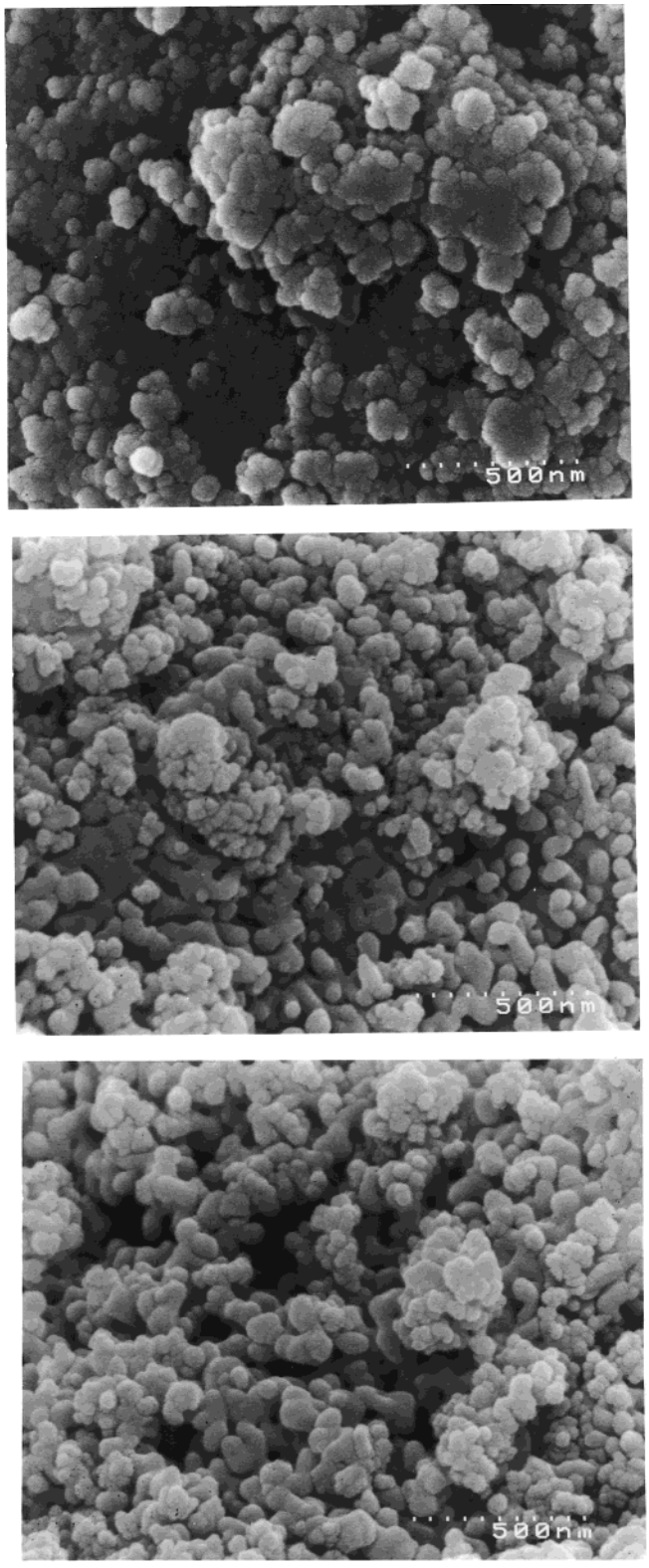

Figure 3. SEM micrographs of the dry precipitate (a, top) and the powders calcined for 2 h at 500 °C (b, middle) and at 700 °C (c, bottom).

(17) Aoyama, T.; Kurata, N.; Hirota, K.; Yamaguchi, O. *J. Am. Ceram. Soc.* **1995**, *78*, 3163.

(18) Li, P.; Chen, I.-W.; Penner−Hahn, J. E. *J. Am. Ceram. Soc.* **1994**, *77*, 1281.

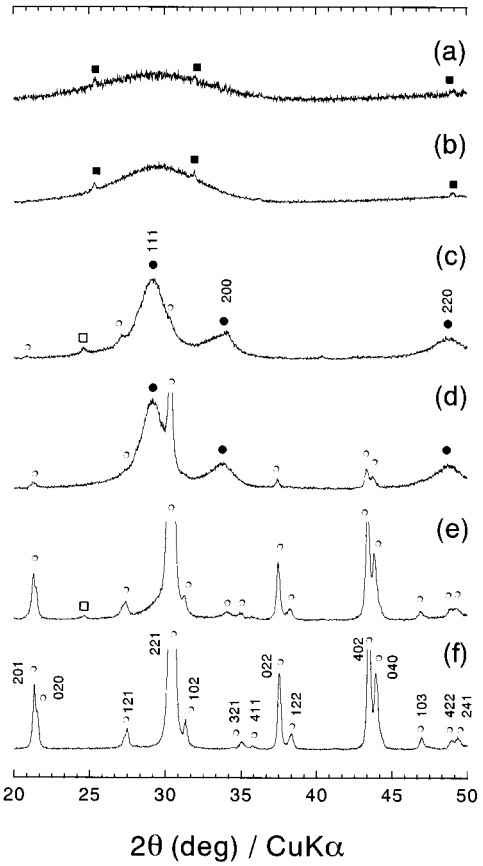

Figure 4. X-ray diffraction patterns of the dry precipitate (a) and of the powders calcined for 2 h at 300 °C (b), 500 °C (c), 550 °C (d), 600 °C (e), and 700 °C (f). The PZ phase is indicated by open circles, the t-Z phase by solid circles, the PbO_2 phase by solid squares, and the PbO phase by open squares. The t-Z phase is indexed in pattern c, and the orthorhombic PZ phase is indexed in pattern f.

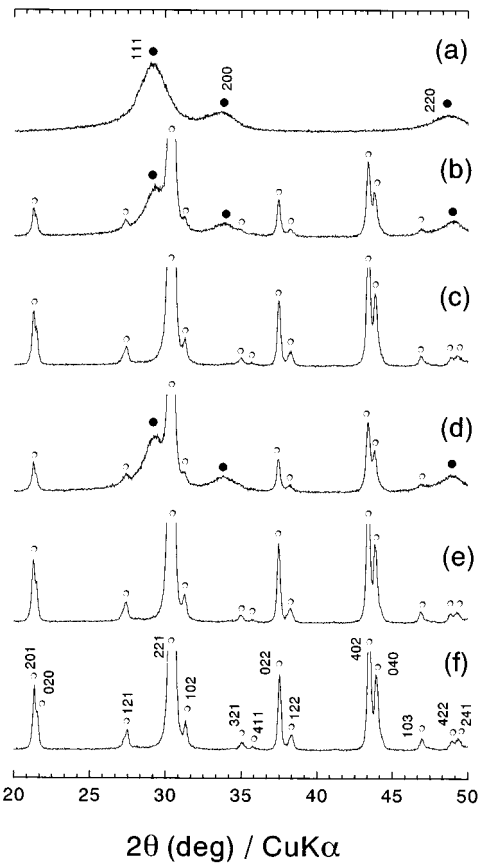

Figure 5. X-ray diffraction patterns of the powders calcined at 600 °C for 5 min (a), 1 h (b), and 8 h (c) and of the powders calcined at 700 °C for 5 min (d), 1 h (e), and 2 h (f). The PZ phase is indicated by open circles and the t-Z phase by solid circles. The t-Z phase is indexed in pattern a, and the orthorhombic PZ phase is indexed in pattern f.

and 48° (indicated by solid circles). This is in agreement with the TG−DTA results (see peak 1 in Figure 2). Although XRD is not sensitive enough to distinguish between the tetragonal and cubic phases of zirconia solid solutions with small particle size, the t-Z phase was identified by Raman spectroscopy (see Figures 6 and 7). The small peak observed at 24.6° (indicated by open squares in Figure 4c) corresponds to the PbO phase, resulting from the decomposition of PbO_2 at elevated temperatures. The PZ phase (indicated by open circles) was identified in the powders calcined at 500 °C and higher temperatures, curves c−f, in agreement with the DTA result (see peak 2 in Figure 2). The main diffraction peaks of the orthorhombic PZ phase were indexed assuming the orthorhombic space group symmetry *Pbam*[20] in the XRD pattern of the powder calcined at 600 °C for 2 h, curve e.

Heat-treatment conditions (temperature and time) play an important role in the crystallization process. Figure 5 shows two series of XRD patterns, for the powders calcined at 600 and 700 °C. The influence of time on the phase formation was observed in the XRD patterns of the powder calcined at 600 °C, curves a−c. In curve a (calcination time 5 min), only the lead-rich t-Z phase (indicated by solid circles) was obtained. Predominantly the PZ phase (indicated by open circles) was observed in curve b (calcination time 1 h). Finally, in the powder calcined at 600 °C for 8 h, curve c, pure orthorhombic PZ was obtained. It is important to remember that when the powder was calcined at 600 °C for 2 h (as discussed above) almost pure PZ was obtained. In the powders calcined at 700 °C (curves d−f in Figure 5) the PZ phase was already observed when the powder was calcined for only 5 min (curve d). In the XRD patterns of the powders calcined for 1 and 2 h, curves e and f, respectively, pure orthorhombic PZ was identified.

3.4. Raman Characterization. Figure 6 shows the Raman spectra of the powders calcined for 2 h between 300 and 900 °C. It is well-known that the Raman spectra of amorphous powders consist of few broad bands, with maxima at roughly the frequencies corresponding to the peaks of the crystalline phase.[21] Two important points can be extracted from spectrum of the powder calcined at 300 °C: (i) the nanometer scale of the PbO_2 particle size, as observed by the broad band at low frequency (indicated by A) and (ii) the absence of the peak at around 130 cm^{-1} (indicated by B_1), which

(19) Yashima, M.; Arashi, H.; Kakihana, M.; Yoshimura, M. *J. Am. Ceram. Soc.* **1994**, *77*, 1067.
(20) Yamasaki, K.; Soejima, Y. *Acta Crystallogr.* **1998**, *B54*, 524.
(21) Brodsky, M. H. In *Light Scattering in Solids I*; Cardona, M., Ed.; Topics in Applied Physics, Vol. 8; Cardona, M., Ed.; Springer: Berlin, Heidelberg, New York, 1975.

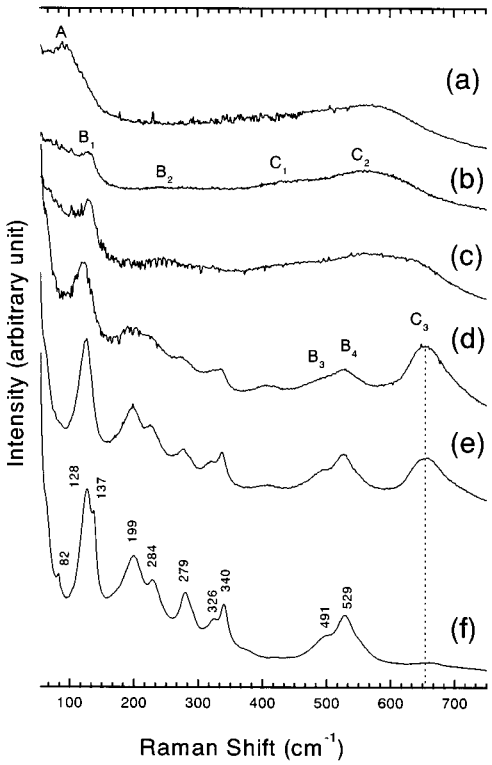

Figure 6. Raman spectra of the powders calcined for 2 h at 300 °C (a), 500 °C (b), 550 °C (c), 600 °C (d), 700 °C (e), and 900 °C (f).

appears only in curves b−f. This was associated with the presence of the PZ phase, in agreement with the TG−DTA and XRD results. The broad band indicated by B_2 was related to the PZ nanoparticles.

As mentioned in the previous section, Raman spectroscopy can be used to distinguish the crystal phases of small particle size zirconium solid solutions, since vibrational modes are strongly dependent on the structure and composition.[19,22] In Raman spectrum b of the powder calcined at 500 °C for 2 h, the presence of two broad bands, indicated by C_1 at around 430 cm^{-1} and C_2 at 570 cm^{-1}, are conclusive evidence of the tetragonal lead-rich structure of the t-Z phase solid solution.[23,24] A typical Raman spectrum of the PZ phase was obtained only when the powders were calcined at 600 °C or at higher temperature, in agreement with the XRD results. The main peaks of the PZ phase are shown in Figure 5f, measured from the powder calcined at 900 °C for 2 h. The peak at around 650 cm^{-1}, indicated by C_3 in curves d−f, was associated with the presence of the t-Z phase. The intensity of this peak decreased with increasing calcination temperature, and was used to estimate the change in the relative amounts of t-Z and PZ phases. The intensities of peaks B_1, B_2, and B_3 of the PZ phase increased with increasing calcination temperature and improvement of the crystal quality.

The relative intensities of these selected peaks are shown in Table 2. We emphasize that the ratios given in Table 2 are not to be interpreted as relative phase fractions, but they merely indicate the change in the phase fractions as a function of calcination temperature. There was no observable influence of the temperature on the relative intensity of the PZ peaks, as indicated by the nearly constant values of the ratios B_2/B_1 and B_3/B_1. The intensity ratio C_3/B_1 approached zero with increasing calcination temperature, indicating that the relative amount of the t-Z phase also decreased. It was possible to observe that the calcination temperature was a more important factor than calcination time. Increasing the calcination time but keeping the temperature constant resulted in a smaller decrease in the C_3/B_1 ratio than increasing the calcination temperature.

Table 2. Relative Intensities of the Selected Raman Peaks of the Powders Calcined under Different Conditions[a]

calcination conditions	C_3/B_1	B_2/B_1	B_3/B_1
600 °C, 2 h	1.3	0.13	0.38
600 °C, 8 h	0.66	0.13	0.38
700 °C, 1 h	0.56	0.15	0.42
700 °C, 2 h	0.48	0.13	0.36
900 °C, 2 h	0.031	0.13	0.38
1000 °C, 2 h	0.000054	0.13	0.35

[a] Peak C_3 at 655 cm^{-1} corresponds to the t-Z phase, and peaks B_1 at 128 cm^{-1}, B_2 at 491 cm^{-1}, and B_3 at 529 cm^{-1} correspond to the PZ phase.

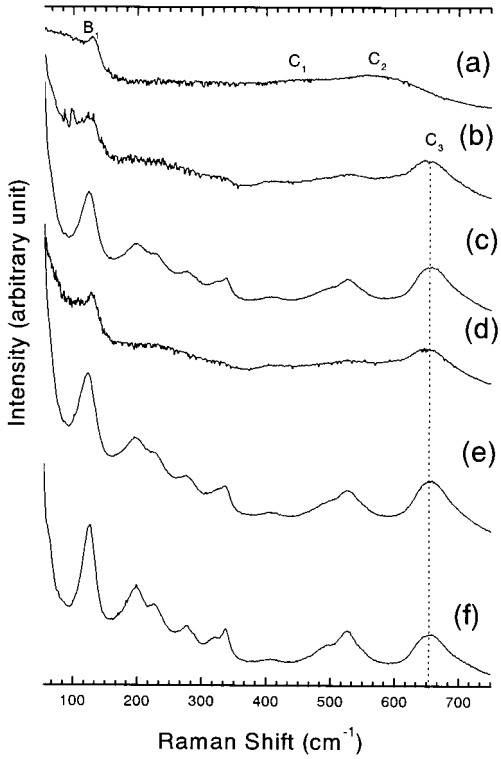

Figure 7. Raman spectra of the powders calcined at 600 °C for 5 min (a), 1 h (b), and 8 h (c) and of the powders calcined at 700 °C for 5 min (d), 1 h (e), and 2 h (f).

Figure 7 shows the influence of time on the Raman spectra of the powders calcined at 600 °C for 5 min, 1 h, and 8 h, curves a−c, respectively, and at 700 °C for 5 min, 1 h, and 2 h, curves d−f, respectively. The most valuable data extracted from Figure 7 are the presence of the PZ phase (peak B_1 in curve a), which could not be detected by X-ray diffraction, probably because of its small amount, and the presence of peak C_3 corresponding to the t-Z phase.

(22) Kakihana, M. *Trends Appl Spectrosc.* **1993**, *1*, 261.
(23) Fujimori, H.; Yashima, M.; Kakihana, M.; Yoshimura, M. *J. Am. Ceram. Soc.* **1998**, *81*, 2885.
(24) Bouvier, P.; Lucazeau, G. *J. Phys. Chem. Solids* **2000**, *61*, 569.

4. Conclusions

Ultrafine $PbZrO_3$ powders with orthorhombic structure were successfully prepared through a new approach of the PBR, which can be called the oxidant−peroxo method. This method results in lead based oxides free from carbon and halides, with a homogeneous microstructure, fine grain distribution of the powders, and nanoscale particle size with an average diameter of 50 nm. The formation of the soluble zirconyl−peroxide complex was supported by the absence of zirconium oxide segregation from the hydrolysis of free zirconyl ion. Although the small segregation of PbO_2 was observed, EDS analysis revealed that Pb and Zr cations were uniformly distributed in the dry precipitate. The PZ phase was first formed at around 500 °C via an intermediate t-Z phase formed at 300 °C. These phases were identified by XRD, Raman spectroscopy, and TG−DTA. The change in the relative amount of the t-Z phase as a function of calcination temperature and time was estimated from the relative intensities of selected Raman peaks.

Acknowledgment. E.R.C. expresses his gratitude to MONBUSHO-Ministry of Education, Science, Sports and Culture of Japan and the Nippon Sheet Glass Foundation for Materials Science and Engineering. This work was financially supported by the "Research for the Future" Program (Grant JSPS-RFTF 96R06901) of the Japan Society for the Promotion of Science (Research Coordinator Prof. Yoshimura of the Tokyo Institute of Technology) and by a Grant-in-Aid for Scientific Research (12555177).

CM010326M